AIAA JOURNAL
Vol. 44, No. 9, September 2006

Stochastic Dynamics of a Nonlinear Aeroelastic System

Seunggil Choi* and N. Sri Namachchivaya†
University of Illinois at Urbana–Champaign, Urbana, Illinois 61801, USA

DOI: 10.2514/1.858

We investigate the asymptotic behaviors of a thin panel in high supersonic flow with a turbulent boundary layer. The objective of this investigation is achieved by formulating methods to analyze complex interactions among aerodynamic/structural dynamic nonlinearities, turbulence, and stability. We reduce an infinite dimensional model to a finite dimensional system in the Galerkin's sense. The normal form technique is employed not only to capture the essential dynamics of the system in which significant nonlinearities are considered but also to reduce the dimensionality of the dynamical system. Because of the random nature of forcing characteristics associated with the turbulence, the theory of stochastic processes is used to explore panel responses in the presence of turbulent boundary layer. After adequate scaling of parameters, a nonstandard reduction through stochastic averaging is achieved. It turns out that the solution of the reduced model is approximated by a Markov process that takes its value on a graph with gluing conditions that furnish the complete specification of the dynamics of the reduced model. With the aid of the infinitesimal generator of the reduced Markov process on the graph, we examine stochastic analyses such as mean exit time, probability density and stochastic bifurcation in the phenomenological sense.

Nomenclature

a	=	panel length
b	=	panel width
c_a	=	speed of sound
D	=	panel bending stiffness, $D = [Eh^3/12(1-\nu^2)]$
E	=	Young's modulus
$\mathcal{E}$	=	linear vector space, $\mathcal{E} = \mathcal{E}_0 \oplus \mathcal{E}_-$
$\mathcal{E}_0$, $\mathcal{E}_-$	=	center subspace, stable subspace
$F(X)$, $N(X, Y)$	=	normal forms in $\mathcal{E}_0$, $\mathcal{E}_-$
G	=	shear modulus
$\mathcal{H}^1$	=	one-dimensional Hausdor measure
h	=	panel thickness
M	=	Mach number
m	=	uniform mass per unit area
N_x^E	=	external axial load
P_0, P_-	=	projections onto $\mathcal{E}_0$, $\mathcal{E}_-$
q	=	dynamic pressure, $q = \rho_a U^2/2$
t	=	time
U	=	air flow speed
u, v, w	=	displacement components in x, y, and z
x, y, z	=	spatial coordinates
γ	=	ratio of specific heat
ν	=	Poisson ratio
ρ_a	=	air density
$\Phi(X, Y)$	=	near identity coordinate transformation
$\|\cdot\|_{T\mathbb{R}^2}$	=	standard metric on $T\mathbb{R}^2$

I. Introduction

AEROELASTICITY studies the mutual interaction between aerodynamic and elastic forces, and the influence of this interaction on the design of high speed flight vehicles. The interaction of aerodynamic forces with flexible structures such as a panel can create complicated vibrational effects that may adversely affect the overall performance of aircraft. Phenomena such as large amplitude flutter, buckling, and fatigue failure are all possible results of flow-induced dynamics (e.g., Dowell [1]). To obviate such occurrences, we need to understand how the flow and structural parameters contribute to aeroelasticity. Dwell and Ilgamov [2] provide a general survey of nonlinear aeroelasticity. Recent work has shown that these nonlinearities play a key role in determining crucial performance characteristics such as flutter amplitude and buckling displacements [3].

Another element that is of considerable importance on the dynamical behavior is pressure fluctuations induced by a turbulent boundary layer (TBL). The TBL-induced vibrations could cause fatigue damage on the structure. Therefore, such fatigue stresses should be taken into consideration in the airplane design. From a mathematical modeling point of view, such pressure fluctuations cannot be adequately described in terms of a deterministic function of time alone. This pressure fluctuates randomly over a wide band of frequencies and might be considered as stochastic functions of time defined only in probabilistic terms. Hence, the probabilistic approach employing the theory of stochastic processes is addressed.

This paper investigates the nonlinear aeroelastic behavior of a thin, flat panel under the TBL in a high supersonic flow through a useful methodology developed here. We extend the work of Namachchivaya and Lee [4], including the effects of the TBL as a random process on the panel dynamics. In addition, we consider the system with nonnegligible aerodynamic dissipation, which implies that the system is no longer *reversible* as in [4].

The random nature of the forcing characteristics associated with the TBL-induced fluctuation is assumed to be stationary and of small magnitude, the effects of which are of significance when the deterministic system is close to bifurcations. It is well known (see Guckenheimer and Holmes [5]) that the panel dynamics exhibit three types of instability, namely, divergence, flutter, and double-zero instability. The most interesting one is associated with the double-zero eigenvalues because it can exhibit the characteristics of both Hopf and simple bifurcation together. Hence, close to such instability, the theory of normal form and stochastic averaging are applied in order to reduce the original problem to a tractable form. These two reduction schemes that are addressed in this paper are based on the equivariant normal form theory of Elphick et al. [6] and nonstandard reduction through stochastic averaging developed by Namachchivaya and Sower [7–9].

This paper is outlined as follows. Section II is devoted to formulating the thin plate mathematical model with aerodynamic and structural nonlinearities. Then we construct finite dimensional evolution (amplitude) equations by using Galerkin's method.

Received 4 March 2003; revision received 11 March 2006; accepted for publication 19 March 2006.

*Research Assistant, Nonlinear Systems Group, Department of Aerospace Engineering.

†Professor, Nonlinear Systems Group, Department of Aerospace Engineering.

Section III presents the characterization of instability boundaries in parameter spaces. Section IV applies the normal form theory to the finite dimensional system close to double-zero instability. Elphick et al. [6] have shown that their method yields both the normal form and the center manifold simultaneously. In Sec. V, the stochastic averaging method is presented. More concretely, we address a separation of time scales so that the state variable of fast time scales can be averaged out while the equation of the slow variables is approximated. The noise induced by the TBL is idealized as a zero mean, independent Gaussian white noise, leading to Ito's stochastic differential equations (SDE's) in the present paper. The nonstandard reduction techniques admit that the solution process of the reduced system converges weakly to the law of Markov process. In Sec. VI, the mean exit time problem is investigated from the reduced Markov process with its averaged generator (limiting generator). The adjoint problem of the limiting generator is formulated for the graph valued process that is developed via the nonstandard reduction technique. Then stationary probability densities are studied by solving the *Fokker–Planck equation* (FPE). Subsequently, we examine stochastic P-bifurcation (*phenomenological approach*), illustrating the long term behavior of the thin panel dynamics.

II. Problem Formulation

To begin with, the plate model shown in Fig. 1 is described by a general nonlinear aeroelastic system in Dowell [10]. The governing partial differential equation (PDE) of motion includes the nonlinear characteristics due to structural geometry such as a nonlinear coupling between in-plane stretching and out-of-plane bending and due to aerodynamic loading and the TBL-induced fluctuation. Since the structural damping induced by internal frictions has little effect on the panel motion, we can neglect the effect of structural dissipation.

$$D\nabla^4 w = (N_x + N_x^E)w_{,xx} + N_y w_{,yy} + 2N_{xy}w_{,xy} - mw_{,tt} - \Delta p^M - \Delta p^E \tag{1}$$

$$N_{x,x} + N_{xy,y} = 0, \qquad N_{xy,x} + N_{y,y} = 0 \tag{2}$$

where $\nabla^4 w \overset{\text{def}}{=} w_{,xxxx} + 2w_{,xxyy} + w_{,yyyy}$, and Δp^M is the aerodynamic pressure induced by the plate motion. Δp^E represents external loadings such as the pressure exerted by the TBL or by other unsteady sources, which can be considered a random function with specific noise characteristics. N_x^E is a direct load in the flow direction.

The expressions for the stress resultants N_x, N_y, and N_{xy} are given as follows:

$$\begin{aligned} N_x &= \frac{Eh}{1-\nu^2}[u_{,x} + \tfrac{1}{2}w_{,x}^2 + \nu v_{,y} + \tfrac{1}{2}\nu w_{,y}^2] \\ N_y &= \frac{Eh}{1-\nu^2}[v_{,y} + \tfrac{1}{2}w_{,y}^2 + \nu u_{,x} + \tfrac{1}{2}\nu w_{,x}^2] \\ N_{xy} &= Gh(v_{,x} + u_{,y} + w_{,x}w_{,y}) \end{aligned} \tag{3}$$

The supersonic flow over the panel generates the pressure difference Δp^M with respect to the cavity below (which we assume is deep enough not to have significant influences such as acoustics on the panel response). For *inviscid high supersonic* flow regimes, the following third-order, quasisteady piston theory approximation (Lighthill [11], Ashley and Zartarian [12]) can be derived as an estimate of Δp^M.

$$\Delta p^M = \frac{2q}{M}\left[\left(\frac{1}{U}w_{,t} + w_{,x}\right) + \frac{1+\gamma}{4}M\left(\frac{1}{U}w_{,t} + w_{,x}\right)^2 + \frac{1+\gamma}{12}M^2\left(\frac{1}{U}w_{,t} + w_{,x}\right)^3\right] \tag{4}$$

Cunningham [13] has shown that this theory gives a good estimate for the aerodynamic loads exposed to high supersonic Mach number flow regimes. Bein et al. [14] also have shown that for high supersonic flow regimes, the third-order, quasisteady piston theory approximation produces unsteady aerodynamic loading that is in close agreement with that based on direct solution of the Euler equations. Hence, the piston theory model considered here included both quadratic and cubic nonlinearities, which is necessary due to the lack of flow under the panel.

We shall consider the pinned boundary conditions for the edges of the plate:

$$\begin{aligned} &x = 0, \quad a{:}u = 0, \quad w = 0, \quad \text{and} \quad w_{,xx} = 0 \\ &y = 0, \quad b{:}v = 0, \quad w = 0, \quad \text{and} \quad w_{,yy} = 0 \end{aligned}$$

Substituting nondimensional parameters into Eqs. (1–3),

$$\begin{aligned} &\bar{w} = w/a, \quad \bar{u} = u/a, \quad \bar{v} = v/a, \quad \xi = x/a \\ &\eta = y/a, \quad \tau = t(D/ma^4)^{1/2}, \quad \lambda = \rho U^2 a^3/MD \\ &\mu = \rho a/m, \quad r = a/b, \quad \delta = h^2/a^2, \quad R_\xi = N_x^E a^2/D \end{aligned}$$

yields the following set of equations

$$\bar{w}_{,\xi\xi\xi\xi} + 2\bar{w}_{,\xi\xi\eta\eta} + \bar{w}_{,\eta\eta\eta\eta} = (N_\xi + R_\xi)\bar{w}_{,\xi\xi} + N_\eta \bar{w}_{,\eta\eta} + 2N_{\xi\eta}\bar{w}_{,\xi\eta} - \bar{w}_{,\tau\tau} - \Delta P^M - \Delta P^E \tag{5}$$

$$N_{\xi,\xi} + N_{\xi\eta,\eta} = 0, \qquad N_{\xi\eta,\xi} + N_{\eta,\eta} = 0 \tag{6}$$

where

$$\begin{aligned} N_\xi &= \frac{12}{\delta}[\bar{u}_{,\xi} + \tfrac{1}{2}\bar{w}_{,\xi}^2 + \nu\bar{v}_{,\eta} + \tfrac{1}{2}\nu\bar{w}_{,\eta}^2] \\ N_\eta &= \frac{12}{\delta}[\bar{v}_{,\eta} + \tfrac{1}{2}\bar{w}_{,\eta}^2 + \nu\bar{u}_{,\xi} + \tfrac{1}{2}\nu\bar{w}_{,\xi}^2] \\ N_{\xi\eta} &= \frac{6(1-\nu)}{\delta}(\bar{v}_{,\xi} + \bar{u}_{,\eta} + \bar{w}_{,\xi}\bar{w}_{,\eta}) \end{aligned} \tag{7}$$

The pressure difference (4) induced by the panel motion can be rewritten in nondimensional form as

$$\Delta P^M = \lambda\left(\delta_P + \frac{1+\gamma}{4}M\delta_P^2 + \frac{1+\gamma}{12}M^2\delta_P^3\right) \tag{8}$$

wherein

$$\delta_P = \sqrt{\frac{\mu}{M\lambda}}\bar{w}_{,\tau} + \bar{w}_{,\xi}$$

The pressure fluctuations induced by the TBL can be expressed as functions of time and spatial coordinates and may be defined by the use of separation of variables: $\Delta P^E = W(\tau)X(\xi,\eta)$.

The nondimensional boundary conditions for a panel with pinned edges become:

$$\begin{aligned} &\xi = 0, \quad 1{:}\bar{u} = 0, \quad \bar{w} = 0, \quad \text{and} \quad \bar{w}_{,\xi\xi} = 0 \\ &\eta = 0, \quad \tfrac{1}{r}{:}\bar{v} = 0, \quad \bar{w} = 0, \quad \text{and} \quad \bar{w}_{,\eta\eta} = 0 \end{aligned}$$

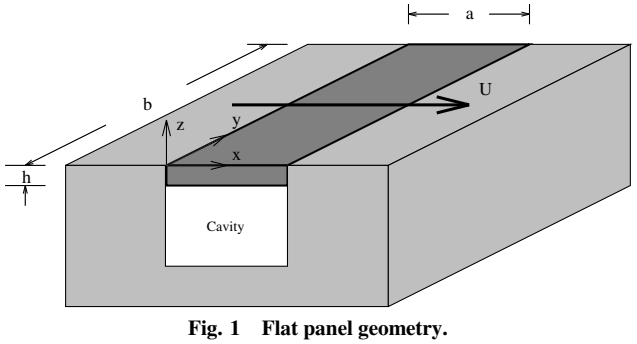

Fig. 1 Flat panel geometry.

Since $\bar{u}, \bar{v} \ll \bar{w}$, we make use of scaling parameter $\delta = (h^2/a^2) \ll 1$ such that $\bar{w} = \delta\bar{w}$, $\bar{u} = \delta^2\bar{u}$, and $\bar{v} = \delta^2\bar{v}$. The set of plate equations at $\mathcal{O}(1)$ from Eqs. (5) and (6) is obtained:

$$\bar{w}_{\tau\tau} + \nabla^4\bar{w} = 0 \tag{9}$$

$$\begin{aligned}
&\bar{u}_{,\xi\xi} + \frac{1-\nu}{2}\bar{u}_{,\eta\eta} + \frac{1+\nu}{2}\bar{u}_{,\xi\eta} + \bar{w}_{,\xi}\bar{w}_{,\xi\xi} + \frac{1-\nu}{2}\bar{w}_{,\xi}\bar{w}_{,\eta\eta} \\
&\quad + \frac{1+\nu}{2}\bar{w}_{,\eta}\bar{w}_{,\xi\eta} = 0, \\
&\bar{v}_{,\eta\eta} + \frac{1-\nu}{2}\bar{v}_{,\xi\xi} + \frac{1+\nu}{2}\bar{u}_{,\xi\eta} + \bar{w}_{,\eta}\bar{w}_{,\eta\eta} + \frac{1-\nu}{2}\bar{w}_{,\eta}\bar{w}_{,\xi\xi} \\
&\quad + \frac{1+\nu}{2}\bar{w}_{,\xi}\bar{w}_{,\xi\eta} = 0
\end{aligned} \tag{10}$$

Hence, the stationary homogeneous solution for $\bar{w}$ of Eq. (9) in the panel with pinned edges reads,

$$\bar{w} = \sum_m \sum_n Z_{mn} \sin(m\pi\xi)\sin(n\pi r\eta) \tag{11}$$

In what follows, we calculate $\bar{u}$ and $\bar{v}$ which satisfy Eq. (6). We first consider only two predominant coupled modes in the air flow direction from Eq. (11) to obtain

$$\bar{w} = z_1(\tau)\sin(m_1\pi\xi)\sin(n_1\pi r\eta) + z_2(\tau)\sin(m_2\pi\xi)\sin(n_2\pi r\eta) \tag{12}$$

Substituting expressions (7) and (12) into Eq. (6) and solving the resulting set of PDE's yields

$$\begin{aligned}
\bar{u} = {}& \tfrac{1}{16}z_1^2 m_1\pi[-1 + \nu n_1^2 r^2/m_1^2 + \cos(2n_1\pi r\eta)]\sin(2m_1\pi\xi) \\
&+ \tfrac{1}{16}z_2^2 m_2\pi[-1 + \nu n_2^2 r^2/m_2^2 + \cos(2n_2\pi r\eta)]\sin(2m_2\pi\xi) \\
&+ z_1 z_2\{c_1\cos[(n_1-n_2)\pi r\eta]\sin[(m_1+m_2)\pi\xi] \\
&+ c_2\cos[(n_1+n_2)\pi r\eta]\sin[(m_1+m_2)\pi\xi] \\
&+ c_3\cos[(n_1-n_2)\pi r\eta]\sin[(m_1-m_2)\pi\xi] \\
&+ c_4\cos[(n_1+n_2)\pi r\eta]\sin[(m_1-m_2)\pi\xi]\}
\end{aligned} \tag{13}$$

$$\begin{aligned}
\bar{v} = {}& \tfrac{1}{16}z_1^2 n_1\pi r[-1 + \nu m_1^2/n_1^2 r^2 + \cos(2m_1\pi\xi)]\sin(2n_1\pi r\eta) \\
&+ \tfrac{1}{16}z_2^2 n_2\pi r[-1 + \nu m_2^2/n_2^2 r^2 + \cos(2m_2\pi\xi)]\sin(2n_2\pi r\eta) \\
&+ z_1 z_2\{c_5\cos[(m_1+m_2)\pi\xi]\sin[(n_1+n_2)\pi r\eta] \\
&+ c_6\cos[(m_1-m_2)\pi\xi]\sin[(n_1+n_2)\pi r\eta] \\
&+ c_7\cos[(m_1+m_2)\pi\xi]\sin[(n_1-n_2)\pi r\eta] \\
&+ c_8\cos[(m_1-m_2)\pi\xi]\sin[(n_1-n_2)\pi r\eta]\}
\end{aligned} \tag{14}$$

The explicit forms of the coefficients and the detailed calculations are given in Lee [15]. In the sequel, we let $n_1 = n_2$ for a simpler case and substitute $\bar{w}$, $\bar{u}$, and $\bar{v}$ into Eq. (5). By applying Galerkin's method [16], one of classical approximation methods for PDE's, we obtain the set of two-dimensional coupled second order ordinary differential equations (ODE's):

$$\ddot{z} + Kz + F(z) + [G^\epsilon\dot{z} + F^\epsilon(z,\dot{z})] + \xi(\tau)\bar{K}z = \nu\eta(\tau) \tag{15}$$

where

$$K = \begin{bmatrix} \omega_1^2 & -\gamma\lambda \\ \gamma\lambda & \omega_2^2 \end{bmatrix}, \qquad G^\epsilon = \begin{bmatrix} \sqrt{\mu\lambda/M} & 0 \\ 0 & \sqrt{\mu\lambda/M} \end{bmatrix}$$

$$\bar{K} = \begin{bmatrix} -m_1^2\pi^2 & 0 \\ 0 & -m_2^2\pi^2 \end{bmatrix}, \qquad \nu = \begin{Bmatrix} \nu_1 \\ \nu_2 \end{Bmatrix}$$

$$\gamma = \frac{2m_1m_2(1-(-1)^{m_1+m_2})}{m_2^2 - m_1^2}, \qquad \Gamma = -R_\xi$$

$$\omega_1^2 = \pi^4(m_1^2 + n^2r^2)^2 - m_1^2\pi^2\Gamma$$

$$\omega_2^2 = \pi^4(m_2^2 + n^2r^2)^2 - m_2^2\pi^2\Gamma$$

$$\nu_i = \int_0^{1/r}\int_0^1 X(\xi,\eta)\sin(m_i\pi\xi)\sin(n\pi r\eta)\,\mathrm{d}\xi\,\mathrm{d}\eta, \quad \text{where } i = 1,2$$

$F(z)$ and $F^\epsilon(z,\dot{z})$ are the nonlinear coefficients of the approximating system. The linear and nonlinear terms $Kz + F(z)$ contain some of the follower-type aerodynamic terms and all of the terms that stem from the nonlinear panel. The damping and velocity dependent aerodynamic terms are given by $G^\epsilon\dot{z} + F^\epsilon(z,\dot{z})$. The term $\xi(\tau)$ represents a *multiplicative noise* that is added to axial load R_ξ whereas $\eta(\tau)$ is an *additive noise* that represents the TBL-induced pressure fluctuation. The coefficients ν_1, ν_2 denote noise intensities.

In what follows, we can rewrite the set of the second order ODE's into the set of the first order ODE's in terms of the state variables which are defined by $x_1 = z_1$, $x_2 = \dot{z}_1$, $x_3 = z_2$, $x_4 = \dot{z}_2$

$$\dot{x}(t) = A_\mu x + F_\mu(x) + \xi(t)Bx + \sigma\eta(t) \tag{16}$$

Here we let $A_\mu = A + A^\epsilon$ and $F_\mu(x) = F(x) + F^\epsilon(x)$, where

$$A = \begin{bmatrix} 0 & 1 & 0 & 0 \\ -\omega_1^2 & 0 & \gamma\lambda & 0 \\ 0 & 0 & 0 & 1 \\ -\gamma\lambda & 0 & -\omega_2^2 & 0 \end{bmatrix}$$

$$A^\epsilon = \begin{bmatrix} 0 & 0 & 0 & 0 \\ 0 & -\sqrt{\mu\lambda/M} & 0 & 0 \\ 0 & 0 & 0 & 0 \\ 0 & 0 & 0 & -\sqrt{\mu\lambda/M} \end{bmatrix}, \qquad F(x) = \begin{Bmatrix} f_1(x) \\ f_2(x) \\ f_3(x) \\ f_4(x) \end{Bmatrix}$$

$$B = \begin{bmatrix} 0 & 0 & 0 & 0 \\ m_1^2\pi^2 & 0 & 0 & 0 \\ 0 & 0 & 0 & 0 \\ 0 & 0 & m_2^2\pi^2 & 0 \end{bmatrix}, \qquad F^\epsilon(x) = \begin{Bmatrix} f_1^\epsilon(x) \\ f_2^\epsilon(x) \\ f_3^\epsilon(x) \\ f_4^\epsilon(x) \end{Bmatrix}$$

$$\sigma = \begin{Bmatrix} \nu_1 \\ \nu_2 \\ \nu_3 \\ \nu_4 \end{Bmatrix}$$

and

$$\begin{aligned}
&f_1(x) = 0, \qquad f_3(x) = 0, \qquad f_1^\epsilon(x) = 0, \qquad f_3^\epsilon(x) = 0 \\
&\qquad \nu_1 = 0, \qquad \nu_3 = 0, \\
&f_2(x) = f_{2,2000}x_1^2 + f_{2,1010}x_1x_3 + f_{2,0020}x_3^2 + f_{2,3000}x_1^3 \\
&\quad + f_{2,2010}x_1^2x_3 + f_{2,1020}x_1x_3^2 + f_{2,0030}x_3^3 \\
&f_4(x) = f_{4,2000}x_1^2 + f_{4,1010}x_1x_3 + f_{4,0020}x_3^2 + f_{4,3000}x_1^3 \\
&\quad + f_{4,2010}x_1^2x_3 + f_{4,1020}x_1x_3^2 + f_{4,0030}x_3^3 \\
&f_2^\epsilon(x) = f_{2,0200}^\epsilon x_2^2 + f_{2,0101}^\epsilon x_2x_4 + f_{2,0002}^\epsilon x_4^2 + f_{2,1101}^\epsilon x_1x_2x_4 \\
&\quad + f_{2,0102}^\epsilon x_2x_4^2 + f_{2,0300}^\epsilon x_2^3 + f_{2,0012}^\epsilon x_3x_4^2 + f_{2,2100}^\epsilon x_1^2x_2 \\
&\quad + f_{2,0120}^\epsilon x_2x_3^2 + f_{2,0210}^\epsilon x_2^2x_3 \\
&f_4^\epsilon(x) = f_{4,0200}^\epsilon x_2^2 + f_{4,0101}^\epsilon x_2x_4 + f_{4,0002}^\epsilon x_4^2 + f_{4,0201}^\epsilon x_2^2x_4 \\
&\quad + f_{4,0003}^\epsilon x_4^3 + f_{4,1200}^\epsilon x_1x_2^2 + f_{4,0021}^\epsilon x_3^2x_4 + f_{4,1002}^\epsilon x_1x_4^2 \\
&\quad + f_{4,0111}^\epsilon x_2x_3x_4 + f_{4,2001}^\epsilon x_1^2x_4
\end{aligned} \tag{17}$$

where the conventional notations of normal form is used as in Namachchivaya et al. [17] and the coefficients $f_{i,jklm}$, $f^{\epsilon}_{i,jklm}$ are given in Lee [15].

III. Characterization of Instability Boundaries for Linear System

This section is devoted to the classification of the possible instabilities that occur as the parameters are varied. The stability of the trivial solution is completely specified by examining the eigenvalues of the linear operator A_μ in Eq. (16). The eigenvalues are obtained by solving the following characteristic equation:

$$\rho^4 + 2\sqrt{\frac{\mu\lambda}{M}}\rho^3 + \left(\frac{\mu\lambda}{M} + \omega_1^2 + \omega_2^2\right)\rho^2 + \sqrt{\frac{\mu\lambda}{M}}(\omega_1^2 + \omega_2^2)\rho + \omega_1^2\omega_2^2 + \gamma^2\lambda^2 = 0 \tag{18}$$

Taking the admissible eigenvalues into account from Eq. (18), the linear system is able to have three critical cases depending on the parameters λ, Γ.

1) The equilibrium has one zero eigenvalue $\rho_1 = 0$ when $\lambda_c = (\sqrt{-\omega_1^2\omega_2^2}/\gamma)$. The remaining three eigenvalues can be solved by setting the last term of Eq. (18) to zero.

2) The equilibrium has a pair of purely imaginary eigenvalues $\rho_{1,2} = \pm i\sqrt{(\omega_1^2 + \omega_2^2)/2}$ when $\lambda_c = [(\omega_1^2 + \omega_2^2)/2\gamma]\{(\mu/2\gamma M) \pm \sqrt{(\mu^2/4\gamma^2M^2) + [(\omega_1^2 - \omega_2^2)/(\omega_1^2 + \omega_2^2)]^2}\}$ and the remaining two eigenvalues are obtained by the equation $\rho^2 + 2\sqrt{\lambda\mu/M}\rho + (\lambda\mu/M) + [(\omega_1^2 + \omega_2^2)/2] = 0$

$$\rho_{3,4} = -\sqrt{\frac{\lambda_c\mu}{M}} \pm i\sqrt{\frac{\omega_1^2 + \omega_2^2}{2}} = -\sqrt{\frac{\lambda_c\mu}{M}} \pm i\pi\sqrt{\frac{\pi^2[(m_1^2 + n^2r^2)^2 + (m_2^2 + n^2r^2)^2] - \Gamma_c(m_1^2 + m_2^2)}{2}} \tag{19}$$

3) The equilibrium has a double zero eigenvalues $\rho_{1,2} = 0$ when

$$\Gamma_c = \frac{\pi^2[(m_1^2 + n^2r^2)^2 + (m_2^2 + n^2r^2)^2]}{m_1^2 + m_2^2} \tag{20}$$

$$\lambda_c = \frac{\pi^4(m_1^2 - m_2^2)^2(m_1^2m_2^2 - n^4r^4)}{2m_1m_2(m_1^2 + m_2^2)[1 - (-1)^{m_1+m_2}]} \tag{21}$$

and the remaining eigenvalues of multiplicity two are given by:

$$\rho_{3,4} = -\sqrt{\frac{\mu\lambda_c}{M}} \tag{22}$$

The stability boundaries for the system are sketched in Fig. 2. Here, we have shown two parameter paths, (1s) indicating an increase in axial load Γ and (2s) indicating an increase in air flow rate λ (the flight speed). The trivial equilibrium point is stable in the region bounded by the curves. The choice of unfolding parameters in the linear operator has a significant effect on the number of calculations involved and the final simplification of the results. We shall now compute linear and nonlinear normal forms at the third case (double zero) in the subsequent section.

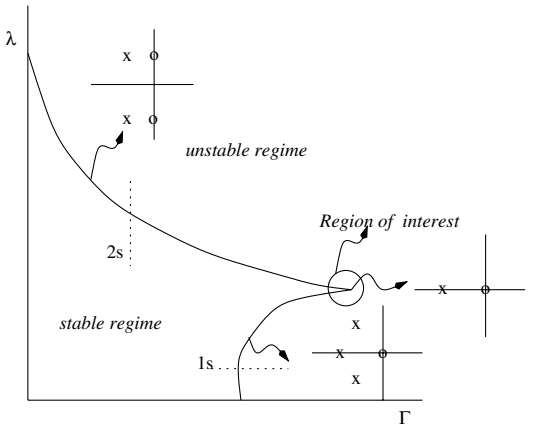

Fig. 2 Linear stability boundary.

IV. Reduction to Normal Form

The normal form theory is to reduce the original system to a simpler model by extracting essential nonlinearities that play a dominant role in the dynamical behavior of the original system. The computation of the normal form is performed, based upon the work of Elphick et al. [6]. This approach employed in this paper yields both the normal form and the center manifold synchronously. The former enables us to eliminate insignificant nonlinearities and the latter to reduce the dimensionality of the original model. The crux of the normal form calculations is to find a homogeneous polynomial vector field of a certain degree in a space complementary to the range of the so-called *homological operator* [18].

To unfold the bifurcation parameters around the critical values of λ_c, Γ_c, we expand the linear operator A_μ and nonlinear term $F_\mu(x)$ in a Taylor series about λ_c, Γ_c. Here the first two leading orders in the linear part and just the first order in the nonlinear part are kept under consideration. Then we transform into Jordan canonical form (or linear normal form) by pre- and postmultiplying the transformation T which comprises a set of eigenvectors. In other words, by substituting $x = T\bar{x}$, we obtain four dimensional ODE close to the double zero and stable eigenvalues as

$$\dot{\bar{x}}(t) = A_{\mu_c}\bar{x} + \mathcal{A}_\mu\bar{x} + F_{\mu_c}(\bar{x}) + \xi(t)\bar{B}\,\bar{x} + \bar{\sigma}\eta(t) \tag{23}$$

where

$$A_{\mu_c} = \begin{bmatrix} 0 & 1 & 0 & 0 \\ 0 & 0 & 0 & 0 \\ 0 & 0 & -\sqrt{\lambda_c\mu/M} & 1 \\ 0 & 0 & 0 & -\sqrt{\lambda_c\mu/M} \end{bmatrix}, \qquad T = \begin{bmatrix} 1 & -\sqrt{\lambda_c\mu/M}/\omega_1^2 & -1/\sqrt{\lambda_c\mu/M} & -1/\omega_1^2 \\ 0 & 1 & 1 & (\sqrt{\lambda_c\mu/M}/\omega_1^2) - (1/\sqrt{\lambda_c\mu/M}) \\ 1 & 0 & -1/\sqrt{\lambda_c\mu/M} & 0 \\ 0 & 1 & 1 & -1/\sqrt{\lambda_c\mu/M} \end{bmatrix}$$

$$\mathcal{A}_\mu = T^{-1}A'T, \qquad \bar{B} = T^{-1}BT, \qquad F_{\mu_c}(\bar{x}) = T^{-1}F_\mu(T\bar{x})$$

$$A' = \frac{\partial}{\partial\Gamma}A_\mu\bigg|_{\Gamma_c,\lambda_c}(\Gamma - \Gamma_c) + \frac{\partial}{\partial\lambda}A_\mu\bigg|_{\Gamma_c,\lambda_c}(\lambda - \lambda_c) = \begin{bmatrix} 0 & 0 & 0 & 0 \\ \pi^2m_1^2(\Gamma - \Gamma_c) & -\frac{1}{2}(\lambda - \lambda_c)\sqrt{\lambda_c\mu/M} & \gamma(\lambda - \lambda_c) & 0 \\ 0 & 0 & 0 & 0 \\ -\gamma(\lambda - \lambda_c) & 0 & \pi^2m_2^2(\Gamma - \Gamma_c) & -\frac{1}{2}(\lambda - \lambda_c)\sqrt{\lambda_c\mu/M} \end{bmatrix}$$

$$\bar{\sigma} = T^{-1}\sigma = \begin{Bmatrix} \{M\sqrt{\lambda_c\mu/M}[\mu\lambda_c\nu_2 + 2M(\nu_1 - \nu_2)\omega_1^2]\}/(\lambda_c\mu)^2 \\ [M(-\nu_1 + \nu_2)\omega_1^2]/\lambda_c\mu \\ \nu_2 + \{[2M(\nu_1 - \nu_2)\omega_1^2]/\lambda_c\mu\} \\ [(\nu_1 - \nu_2)\omega_1^2]/\sqrt{\lambda_c\mu/M} \end{Bmatrix}, \qquad \begin{Bmatrix} x_1 \\ x_2 \\ x_3 \\ x_4 \end{Bmatrix} = \begin{Bmatrix} \bar{x}_1 - (\bar{x}_2\sqrt{\lambda_c\mu/M}/\omega_1^2) - (\bar{x}_3/\sqrt{\lambda_c\mu/M}) - (\bar{x}_4/\omega_1^2) \\ \bar{x}_2 + \bar{x}_3 + \bar{x}_4[-(1/\sqrt{\lambda_c\mu/M}) + (\sqrt{\lambda_c\mu/M}/\omega_1^2)] \\ \bar{x}_1 - (\bar{x}_3/\sqrt{\lambda_c\mu/M}) \\ \bar{x}_2 + \bar{x}_3 - (\bar{x}_4/\sqrt{\lambda_c\mu/M}) \end{Bmatrix}$$

We first carry out the calculation of the linear normal form (*a miniversal deformation or universal unfolding*) of matrix $\mathcal{A}_\mu$ in Eq. (52). The idea is to find the minimum number of parameters (or perturbations) of matrices having the same eigenvalues. In the case of a double zero eigenvalues with nonsemisimple and no further degeneracy, two parameters are required for a complete universal unfolding. Physically, all possible bifurcations that take place in the neighborhood of this bifurcation point will be obtained by making use of these unfolding parameters. The reader is referred to as Wiggins [19] for further discussion. Thus the miniversal deformation is found as

$$A(\lambda) = \begin{bmatrix} 0 & 1 \\ 0 & 0 \end{bmatrix} + \begin{bmatrix} 0 & 0 \\ \lambda_1 & \lambda_2 \end{bmatrix} \tag{24}$$

where λ_1 and λ_2 denote the unfolding parameters that are determined by the fact of having the identical eigenvalues. The details are given in Choi [20]. It is remarked that in view of those unfoldings, it is referred to *local codimension* 2 bifurcations problem.

In the sequel, the general setting for the computation of the nonlinear normal form can be given as follows:

$$\begin{gathered} \dot{Z} = A_{\mu_c} Z + \sum_{k\geq 2} \mathcal{F}_k[Z^{(k)}], \qquad Z = X + Y + \Phi(X, Y) \\ X \in \mathcal{E}_0, Y \in \mathcal{E}_-, Z \in \mathcal{E} \\ \frac{\mathrm{d}X}{\mathrm{d}t} = L_0 X + F(X) + \mathcal{O}((|\,X\,| + |Y|)^p) \\ \frac{\mathrm{d}Y}{\mathrm{d}t} = L_- Y + N(X, Y) + \mathcal{O}(|X|^p) \end{gathered} \tag{25}$$

where

$$\begin{gathered} \Phi(X, Y) = \mathcal{O}(((|X| + |Y|)^2), \qquad F(X) = \mathcal{O}(|X|^2) \\ N(X, Y) = \mathcal{O}(|Y|(|X| + |Y|)) \end{gathered}$$

In this setting, it is to find the normal form $F(X)$ as simple as possible. Based on the computation of Elphick et al. [6], the final normal forms turn out to be

$$\begin{aligned} \begin{Bmatrix} \dot{y}_1 \\ \dot{y}_2 \\ \dot{y}_3 \\ \dot{y}_4 \end{Bmatrix} &= \begin{bmatrix} 0 & 1 & 0 & 0 \\ 0 & 0 & 0 & 0 \\ 0 & 0 & -\sqrt{\lambda_c \mu / M} & 1 \\ 0 & 0 & 0 & -\sqrt{\lambda_c \mu / M} \end{bmatrix} \begin{Bmatrix} y_1 \\ y_2 \\ y_3 \\ y_4 \end{Bmatrix} \\ &+ \begin{bmatrix} 0 & 0 & 0 & 0 \\ \lambda_1 & \lambda_2 & 0 & 0 \\ C_{31} & C_{32} & C_{33} & C_{34} \\ C_{41} & C_{42} & C_{43} & C_{44} \end{bmatrix} \begin{Bmatrix} y_1 \\ y_2 \\ y_3 \\ y_4 \end{Bmatrix} + \begin{Bmatrix} 0 \\ a_0 y_1^2 + b_0 y_1 y_2 \\ f_3^2(y) \\ f_4^2(y) \end{Bmatrix} \\ &+ \begin{Bmatrix} 0 \\ a_1 y_1^3 + b_1 y_1^2 y_2 \\ f_3^3(y) \\ f_4^3(y) \end{Bmatrix} + \begin{Bmatrix} \bar{\sigma}_1 \\ \bar{\sigma}_2 \\ \bar{\sigma}_3 \\ \bar{\sigma}_4 \end{Bmatrix} \eta(t) \end{aligned} \tag{26}$$

where C_{ij} and $f_i^j(y)$, respectively, denote the linear normal form and nonlinear normal form in $\mathcal{E}_-$. Let us remark that C_{ij} and $f_i^j(y)$ simply correspond to the perturbed linear term and the nonlinear terms themselves in the original system Eq. (23) since we have chosen the case that $P_-\Phi_{pq} = 0$. It should be also noted that $\Phi(X, Y)$ gives rise to additional nonlinear terms higher than polynomials of degree of 2, that is the original nonlinear terms are modified by adding the "generated" nonlinear terms. We have taken three factors into account to obtain expression (26). First, we considered only the additive noise $\eta(t)$. Second, the higher order nonlinearities than the polynomials of degree 3 were truncated. Finally, new noise terms of higher order which are created during the process of the coordinates' transformations were assumed very small. It is worth noting that Eq. (26) becomes decoupled between y_1, y_2 and y_3, y_4. In our work, the dynamical behavior of interest is investigated in the center manifold because the behavior in the stable manifold is attracted to the center manifold over a long time. Therefore, we take the first two rows from Eq. (26) into consideration to obtain

$$\begin{aligned} \begin{Bmatrix} \dot{u} \\ \dot{v} \end{Bmatrix} &= \begin{bmatrix} 0 & 1 \\ \mu_1 & \mu_2 \end{bmatrix} \begin{Bmatrix} u \\ v \end{Bmatrix} + \begin{Bmatrix} 0 \\ a_0 u^2 + b_0 uv \end{Bmatrix} \\ &+ \begin{Bmatrix} 0 \\ au^3 + bu^2 v \end{Bmatrix} + \begin{Bmatrix} \nu_1 \\ \nu_2 \end{Bmatrix} \xi(t) \end{aligned} \tag{27}$$

where for the sake of notational clarity, the variables were replaced as follows:

$$\begin{gathered} \lambda_1, \lambda_2 \to \mu_1, \mu_2, \qquad y_1, y_2 \to u, v, \qquad a_1, b_1 \to a, b \\ \eta(t) \to \xi(t), \qquad \bar{\sigma}_1, \bar{\sigma}_2 \to \nu_1, \nu_2 \end{gathered}$$

Let us remark that the set of Eq. (27) includes the quadratic and cubic nonlinearities. The quadratic terms take place due to the effect of the cavity below the panel and the cubic terms account for stretching of the midplane of the panel. The detailed specifications of the coefficients are given in Choi [20]. The rest of the analysis is based on Eq. (27).

V. Nonstandard Reduction

The nonstandard reduction through stochastic averaging for Hamiltonian systems with multiple fixed points is discussed in this section. Appropriate scaling of parameters leads the system (27) to a near integrable Hamiltonian system with certain nontrivial types of fixed points. Then, under small perturbations, the first integral (Hamiltonian or energy) evolves slowly and stochastic averaging makes use of the integrable structure to identify a reduced diffusive model on a space which encodes the structure of the fixed points and can have dimensional singularities. At these singularities, *gluing condition* will be derived, thereby completing the specification of the dynamics of the reduced model. The trajectories of the unperturbed nonlinear system represent the fast variables for which an occupation measure can be easily computed (these occupation measures are used to find the coefficients of the limiting dynamics). The stochastic averaging method addressed here carries the full dynamical feature over to the approximate dynamics of two-dimensional system in the center manifold. In other words, the full dynamics in phase space is projected onto the state space of the energy coordinate H. Thus, we cannot unfold the detailed dynamics in each of energy-level sets.

A. Statement of the Problem

To reduce the number of distinct cases of parameters to be studied, we conduct a rescaling in Eq. (27). Accordingly, we can make the coefficients $a = \pm 1$ and $b = -1$ without loss of generality

$$\begin{aligned} \dot{u} &= v + \nu_1 \xi(t) \\ \dot{v} &= \mu_1 u \pm u^3 + a_0 u^2 + (\mu_2 + b_0 u - u^2) v + \nu_2 \xi(t) \end{aligned} \tag{28}$$

we write Eq. (28) in a weakly perturbed Hamiltonian representation that embraces strong nonlinearities by means of the standard rescaling [5], assuming the additive noise $\xi(t)$ as a *mean zero, stationary, independent, Gaussian white noise*:

$$\begin{gathered} u = \epsilon x, \qquad v = \epsilon^2 y, \qquad \mu_1 = \epsilon \bar{\mu}_1, \qquad \mu_2 = \epsilon^2 \bar{\mu}_2 \\ \nu_1 = \epsilon^2 \bar{\nu}_1, \qquad \nu_2 = \epsilon^3 \bar{\nu}_2, \qquad a_0 = \epsilon \bar{a}_0 \\ b_0 = \epsilon \bar{b}_0, \qquad \bar{t} = \epsilon t \end{gathered}$$

By omitting the bars and putting things in an appropriate mathematical setting, we obtain in a standard form

$$\begin{aligned} \mathrm{d}\hat{Z}_t^\varepsilon &= \{\bar{\nabla}H(\hat{Z}_t^\varepsilon) + \varepsilon b(\hat{Z}_t^\varepsilon)\}\,\mathrm{d}t + \sqrt{\varepsilon}\sigma(\hat{Z}_t^\varepsilon)\,\mathrm{d}W_t \\ \hat{Z}_0^\varepsilon &= z \overset{\text{def}}{=} (x,y)^T \in \mathbb{R}^2 \end{aligned} \tag{29}$$

where

$$\bar{\nabla}H = \begin{Bmatrix} \partial H/\partial y \\ -\partial H/\partial x \end{Bmatrix}, \qquad b(x,y) = \begin{Bmatrix} 0 \\ (\mu_2 + b_0 x - x^2)y \end{Bmatrix} \qquad \sigma(x,y) = \begin{Bmatrix} \nu_1 \\ \nu_2 \end{Bmatrix} \tag{30}$$

The order of $\sqrt{\varepsilon}$ in Eq. (29) was created by the property [21] such that when the process W_t is a standard Brownian motion, and so is the scaled process $(1/\sqrt{\varepsilon})/W_{\varepsilon t}$. In what follows, the corresponding set of the unperturbed flow is given by

$$\begin{aligned} &\dot{\jmath}_t(z) = \bar{\nabla}H[\jmath_t(z)], \qquad \jmath_0(z) = z \in \mathbb{R}^2 \\ &\text{with } H[\jmath_t(z)] \overset{\text{def}}{=} \frac{y^2}{2} - \mu_1\frac{x^2}{2} - a_0\frac{x^3}{3} \mp \frac{x^4}{4} \end{aligned} \tag{31}$$

Let us note that Eq. (31) is perturbed by a small intensity random diffusive motion whose effects can be described via a diffusive *generator*, that is For each test function f and g in $C_b^2(\mathbb{R}^2)$,

$$\mathcal{L}f(z) \overset{\text{def}}{=} \frac{1}{2}\sum_{i,j} a_{i,j}(z)\frac{\partial^2 f}{\partial z_i \partial z_j}(z) + \sum_i b_i(z)\frac{\partial f}{\partial z_i}(z) \tag{32}$$

The associated *symbol* are defined by

$$\langle \mathrm{d}f, \mathrm{d}g\rangle(z) \overset{\text{def}}{=} \sum_{i,j} a_{i,j}(z)\frac{\partial f}{\partial z_i}(z)\frac{\partial g}{\partial z_j}(z) \tag{33}$$

for all $z = (z_1, z_2) \in \mathbb{R}^2$ and $t \geq 0$, where $a_{i,j}(z) \overset{\text{def}}{=} [\sigma(z)\sigma^T(z)]_{ij}$.

Further, it turns out that in order to observe the behavior of the energy level $H(\hat{Z}_t^\varepsilon)$, we need to extend the time interval up to at least ε^{-1}. It is because in view of a new equation for H using Ito's formula

$$\mathrm{d}\,H(\hat{Z}_t^\varepsilon) = \varepsilon(\mathcal{L}H)(\hat{Z}_s^\varepsilon)\,\mathrm{d}t + \sqrt{\varepsilon}(\nabla H, \sigma)(\hat{Z}_s^\varepsilon)\,\mathrm{d}W_s \tag{34}$$

it is evident that the variation of $H(\hat{Z}_t^\varepsilon)$ moves slowly compared with that of $\hat{Z}_t^\varepsilon$. Accordingly, the *averaging principle* can be applied to reduce the system over a long time. Specifically, in a two-dimensional case, we have fast motion around the level sets of H and slow motions across energy levels: the invariant measure of the fast motion of the unperturbed Hamiltonian is a weighted one-dimensional Hausdorff measure. The slow motion (H) across the unperturbed trajectories is approximated by a Markov process through the stochastic averaging method, which was shown by Namachchivaya et al. [7,8,22].

B. Stochastic Averaging on a Graph

In this subsection, we present the calculation of the stochastic averaging on a graph based on the main result [7,8]. Such averaging technique to include multiple fixed points one of which is connected to itself by a homoclinic orbit are given by Freidlin and Wentzell [23]. In such a case, the reduced Markov process takes its values on a graph with certain gluing conditions at the vertices of the graph. These conditions allow the complete description of the limiting behavior of energy-level sets and a unified treatment of the problem in the entire domain. To observe the slow motion H, we extend the time interval up to ε^{-1} to obtain

$$\begin{aligned} \mathrm{d}Z_t^\varepsilon &= \left\{\frac{1}{\varepsilon}\bar{\nabla}H(Z_t^\varepsilon) + b(Z_t^\varepsilon)\right\}\mathrm{d}t + \sigma(Z_t^\varepsilon)\,\mathrm{d}W_t \\ Z_0^\varepsilon &= z \in \mathbb{R}^2, \qquad t \geq 0 \end{aligned} \tag{35}$$

Here, we have made use of the fact that the law of $\{Z_t^\varepsilon; t \geq 0\}$ is the same as the law of $\{\hat{Z}_{t/\varepsilon}^\varepsilon; t \geq 0\}$. It is clear that Z_t^ε defined in Eq. (35) is a Markov process on $\mathbb{R}^2$, whose generator is defined as

$$(\mathcal{L}^\varepsilon\phi)(z) \overset{\text{def}}{=} \mathcal{L}\phi(z) + \frac{1}{\varepsilon}(\bar{\nabla}H, \nabla\phi)(z) \tag{36}$$

with domain $\mathcal{D}(\mathcal{L}^\varepsilon) = \mathbf{C}_b^2(\mathbb{R}^2)$.

We construct a new set of process for the Hamiltonian H as a test function by means of *Ito's formula*

$$M_t = H(Z_t^\varepsilon) - H(z) - \int_0^t \mathcal{L}^\varepsilon H(Z_s^\varepsilon)\,\mathrm{d}s \tag{37}$$

where $M_t = \int_0^t (\nabla H, \sigma)(Z_s^\varepsilon)\,\mathrm{d}W_s$ and M_t is a martingale with quadratic variation

$$\langle M_t\rangle = \int_0^t \langle \mathrm{d}H, \mathrm{d}H\rangle(Z_s^\varepsilon)\,\mathrm{d}s$$

Now, we introduce another test function f, leading to another set of the process through Ito's formula

$$\mathbf{M}_t^f = f\{H(Z_t^\varepsilon)\} - f\{H(z)\} - \int_0^t (\mathbf{L}f)H(Z_s^\varepsilon)\,\mathrm{d}s \tag{38}$$

where $\mathbf{M}_t^f = \int_0^t [\nabla f, (\nabla H, \sigma)](Z_s^\varepsilon)\,\mathrm{d}W_s$. Thus, the infinitesimal generator $\mathbf{L}$ is given by

$$\mathbf{L}\,f[H(Z_t^\varepsilon)] = (\mathcal{L}^\varepsilon H)f' + \tfrac{1}{2}\langle \mathrm{d}H, \mathrm{d}H\rangle f'' \tag{39}$$

where

$$\begin{aligned} \mathcal{L}^\varepsilon H &= Q_{1,2}\cdot G + \tfrac{1}{2}\nu_1^2\cdot M_{1,2} + \tfrac{1}{2}\nu_2^2 \\ \langle \mathrm{d}H, \mathrm{d}H\rangle &= \nu_1^2\cdot N_{1,2}^2 + \nu_1\cdot\nu_2\cdot N_{1,2}\sqrt{Q_{1,2}} + \tfrac{1}{2}\nu_2^2\cdot Q_{1,2} \end{aligned} \tag{40}$$

$$\begin{aligned} Q_{1,2}(x,H) &= 2[H - P_{1,2}(x)] = y^2 \\ P_{1,2}(x) &= -\mu_1\frac{x^2}{2} - a_0\frac{x^3}{3} \mp \frac{x^4}{4}, \qquad G(x) = \mu_2 + b_0 x - x^2 \\ M_{1,2}(x) &= -\mu_1 - 2a_0 x \mp 3x^2, \qquad N_{1,2}(x) = -\mu_1 x - a_0 x^2 \mp x^3 \\ H &= \frac{y^2}{2} + P_{1,2}(x) \end{aligned} \tag{41}$$

The subscripts (1,2) denote the coefficient $a = +1$ and $a = -1$, respectively, and f' represents the differentiation with respect to H.

Now we are concerned with the most interesting case that the unfolding parameter $\mu_1 > 0$ and the coefficient $a = -1$, which implies that the unperturbed Hamiltonian possesses multiple fixed points one of which is connected to itself by a homoclinic orbit. The minimal vertices b_1, b_2 can be easily calculated as

$$\begin{aligned} b_1 &= -\frac{1}{8}\mu_1 d_1^2 - \frac{1}{24}a_0 d_1^3 + \frac{1}{64}d_1^4, \\ b_2 &= -\frac{1}{8}\mu_1 d_2^2 - \frac{1}{24}a_0 d_2^3 + \frac{1}{64}d_2^4 \end{aligned} \tag{42}$$

where $d_1 = a_0 + \sqrt{a_0^2 + 4\mu_1}$ and $d_2 = a_0 - \sqrt{a_0^2 + 4\mu_1}$.

Let us introduce some of terminologies of necessity in order to describe the reduced state space $\bar{\mathcal{I}}$. First, let us introduce the equivalence relation on the original state space $\bar{S}$ which is defined by

$$S \overset{\text{def}}{=} \{x \in \mathbb{R}^2 \colon H(x) < H^*\}$$

It is said that x and y in $\bar{S}$ are equivalent, that is $x \sim y$ if $\jmath_t(x) = y$ for some $t \in \mathbb{R}$. So if $x \in \bar{S}$, we let $[x] \overset{\text{def}}{=} \{y \in \bar{S} \colon y \sim x\}$ be the equivalence class of x. The nonstandard reduction through stochastic averaging enables us to decompose the original state space into a collection of open manifolds such as edges and points. For each of the edges we can define the corresponding 1-dimensional diffusive generator and for each of the saddle points we need to glue the associated generators at the point together. The reduced state space can be given by a graph $\bar{\mathcal{I}} = \bigcup_{i=0}^2 [\mathfrak{c}_i] \cup \bigcup_{i=1}^3 \Gamma_i \cup \circledast$, in Fig. 3,

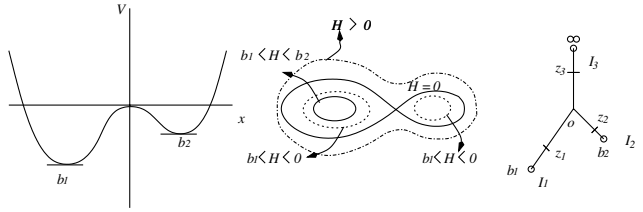

a) Potential function **b) Phase portrait** **c) Graph**

Fig. 3 Schematic of stochastic averaging ($a = -1$, $\mu_1 > 0$, and $a_0 < 0$).

where

$$\Gamma_1 \stackrel{\text{def}}{=} \cup_{\substack{x=(x_1,x_2)\in\bar{S} \\ H(x)<0 \\ x\neq c_1 \\ x_1<0}} [x], \qquad \Gamma_2 \stackrel{\text{def}}{=} \cup_{\substack{x=(x_1,x_2)\in\bar{S} \\ H(x)<0 \\ x\neq c_2 \\ x_1>0}} [x], \qquad \Gamma_3 \stackrel{\text{def}}{=} \cup_{\substack{x=(x_1,x_2)\in\bar{S} \\ H(x)>0}} [x] \tag{43}$$

and c_0 is a saddle at the origin and c_1, c_2 are centers along x axis and as $H^* \to \infty$, $\circledast$ indicates the boundary at ∞ in the reduced state space.

According to main results [7,8], the limiting process on each edge is approximated by a diffusive Markov process with the limiting generator:

$$\begin{aligned}(\mathcal{L}^\dagger f^\dagger)([x]) &\stackrel{\text{def}}{=} \mathcal{L}_i^\dagger f_i(H) \stackrel{\text{def}}{=} \mathbb{A}[\mathbf{L}_i f_i(H)] \\ &= \bar{A}_i(H) f_i' + \tfrac{1}{2}\bar{\sigma}_i^2(H) f_i'' \qquad [x] \in \Gamma_i\end{aligned} \tag{44}$$

where the averaging operator is defined as

$$(\mathbb{A}\varphi)([x]) \stackrel{\text{def}}{=} \frac{\int_{y\in[x]} \varphi(y)\|\bar{\nabla}H(y)\|^{-1}_{T\mathbb{R}^2}\mathcal{H}^1(\mathrm{d}y)}{\int_{y\in[x]} \|\bar{\nabla}H(y)\|^{-1}_{T\mathbb{R}^2}\mathcal{H}^1(\mathrm{d}y)} = \frac{\int_0^{T([x])} \varphi[\partial_s(x)]\,\mathrm{d}s}{T([x])} \qquad \forall\ x \in \bar{\mathcal{S}}c_i] \tag{45}$$

and the return time of the unperturbed flow is defined as

$$T([x]) \stackrel{\text{def}}{=} \inf\{t > 0 \colon \partial_t(x) = x\} = \int_{y\in[x]} \|\bar{\nabla}H(y)\|^{-1}_{T\mathbb{R}^2}\mathcal{H}^1(\mathrm{d}y) \tag{46}$$

The domain of the averaged generator (44) is given by

$$\mathcal{D}(\mathcal{L}^\dagger) \stackrel{\text{def}}{=} \left\{ f^\dagger \in C(\bar{\mathcal{I}}) \colon f^\dagger \in C^2(\cup_{i=1}^3 \Gamma_i), \lim_{H\to H(\mathcal{O})} \mathcal{L}_i^\dagger \text{exist}, \sum_{i=1}^3 (\pm)\sigma_i^2(\mathcal{O}) f_i'(\mathcal{O}) = 0 \right\} \tag{47}$$

where $f_i'(\mathcal{O}) = \lim_{H\to H(\mathcal{O})} f_i'(H)$ for $(H, i) \in I_i$ and the $\pm$ sign denotes whether the coordinate H on the edge I_i is *greater than or less than* $H(\mathcal{O})$. In Eq. (47), the gluing condition for the vertex $\mathcal{O}$

$$\sum_{i=1}^3 (\pm)\sigma_i^2(\mathcal{O}) f_i'(\mathcal{O}) = 0 \tag{48}$$

that corresponds to the saddle point, roughly means the following. Let us define

$$\Delta \stackrel{\text{def}}{=} \sigma_1^2(\mathcal{O}) + \sigma_2^2(\mathcal{O}) + \sigma_3^2(\mathcal{O})$$

If the limiting process starts in edge I_1 of the graph $\bar{\mathcal{I}}$, it evolves according to Eq. (44) with $i = 1$. Upon reaching the vertex, it flips a three-sided coin to decide where it would be headed next. It will go back to edge I_1 with likelihood $\sigma_1^2(\mathcal{O})/\Delta$, to edge I_2 with likelihood $\sigma_2^2(\mathcal{O})/\Delta$, and to edge I_3 with likelihood $\sigma_3^2(\mathcal{O})/\Delta$. Once it is placed in any of three edges, it will evolve according to Eq. (44) with the corresponding σ_i and A_i. When it again hits the vertex $\mathcal{O}$, the coin-flipping procedure is iterated (with a new coin).

It should be noted that H is only a local coordinate in each edge and it can take the same value for different trajectories. The averaged drift and diffusion terms in Eq. (44) are given as follows:

$$\begin{aligned}
\bar{A}_i(H) &= \frac{1}{T_i(H)} \int_0^{T_i(H)} [Q(x,H)G(x) + \tfrac{1}{2}\nu_1^2 M(x) + \tfrac{1}{2}\nu_2^2]\,\mathrm{d}t \\
&\stackrel{\text{def}}{=} \frac{1}{T_i(H)} A_i(H) \\
A_i(H) &= 2\int_{x_i^-(H)}^{x_i^+(H)} [Q(x,H)G(x) + \tfrac{1}{2}\nu_1^2 M(x) + \tfrac{1}{2}\nu_2^2] \frac{\mathrm{d}x}{\sqrt{Q(x,H)}} \\
\bar{\sigma}_i^2(H) &= \frac{1}{T_i(H)} \int_0^{T_i(H)} [\tfrac{1}{2}\nu_1^2 N^2(x) + \tfrac{1}{2}\nu_2^2 Q(x,H) \\
&\quad + \nu_1\nu_2 N(x)(\pm)\sqrt{Q(x,H)}]\,\mathrm{d}t \stackrel{\text{def}}{=} \frac{1}{T_i(H)} \sigma_i^2(H) \\
\sigma_i^2(H) &= 2\int_{x_i^-(H)}^{x_i^+(H)} [\tfrac{1}{2}\nu_1^2 N^2(x) + \tfrac{1}{2}\nu_2^2 Q(x,H)] \frac{\mathrm{d}x}{\sqrt{Q(x,H)}} \\
T_i(H) &= \int_0^T \mathrm{d}t = 2\int_{x_i^-(H)}^{x_i^+(H)} \frac{\mathrm{d}x}{\sqrt{Q(x,H)}}
\end{aligned} \tag{49}$$

where $x_i^{(\pm)}$ are the points where the periodic orbit intersects the x axis, that is the points where $y = 0$. For notational convenience, we dropped the subscripts (1,2) in Eq. (41). To make the averaging calculation easier, the path integral is utilized instead of the integration in the time domain. However, it would work only if the period of the trajectory associated with the corresponding energy level is finite except for homoclinic orbits.

For different values of H, we will have different path integrals and thus different drift $\bar{A}_i(H)$ and diffusion $\bar{\sigma}_i(H)$. For the edges I_1 and I_2, the corresponding integrals are calculated along the paths that correspond to the oscillations. For the edge I_3, the integral is calculated along the paths that correspond to the rotations. The integrals can be expressed in terms of *elliptic integrals* [24]. The drift and diffusion coefficients for each edge can be calculated in terms of the *complete elliptic integrals*.

1a) Edge I_1 ($b_2 < H < 0$):

$$\begin{aligned}
A_1(H) &= f_{11}F(k_1) + f_{12}E(k_1) + f_{13}\Pi(\alpha_1^2, k_1) \\
\sigma_1^2(H) &= g_{11}F(k_1) + g_{12}E(k_1) + g_{13}\Pi(\alpha_1^2, k_1) + g_{14} \\
T_1(H) &= 2\sqrt{2}g_1 \cdot F(k_1)
\end{aligned} \tag{50}$$

1b) Edge I_1 ($b_1 < H \le b_2$):

$$\begin{aligned}
A_1'(H) &= f_{11}'F(k_1') + f_{12}'E(k_1') + f_{13}'\Pi\left(\frac{(\alpha')_1^2}{(\alpha')_1^2 - 1}, k_1'\right) \\
(\sigma')_1^2(H) &= g_{11}'F(k_1') + g_{12}'E(k_1') + g_{13}'\Pi\left(\frac{(\alpha')_1^2}{(\alpha')_1^2 - 1}, k_1'\right) + g_{14}' \\
T_1'(H) &= 4\sqrt{2}g_1' \cdot F(k_1')
\end{aligned} \tag{51}$$

2) Edge I_2 ($b_2 \le H < 0$):

$$\begin{aligned}
A_2(H) &= f_{21}F(k_2) + f_{22}E(k_2) + f_{23}\Pi(\alpha_2^2, k_2), \\
\sigma_2^2(H) &= g_{21}F(k_2) + g_{22}E(k_2) + g_{23}\Pi(\alpha_2^2, k_2) + g_{24}, \\
T_2(H) &= 2\sqrt{2}g_2 \cdot F(k_2)
\end{aligned} \tag{52}$$

3) Edge I_3 ($H > 0$):

$$\begin{aligned}
A_3(H) &= f_{31}F(k_3) + f_{32}E(k_3) + f_{33}\Pi\left(\frac{\alpha_3^2}{\alpha_3^2 - 1}, k_3\right), \\
\sigma_3^2(H) &= g_{31}F(k_3) + g_{32}E(k_3) + g_{33}\Pi\left(\frac{\alpha_3^2}{\alpha_3^2 - 1}, k_3\right) + g_{34}, \\
T_3(H) &= 4\sqrt{2}g_3 \cdot F(k_3)
\end{aligned} \tag{53}$$

where

$$f_{1j} = f_{1j}(k_1, g_1, \alpha_1, \alpha_1', x_1^-, x_1^+, x_2^-, x_2^+),$$
$$g_{1j} = g_{1j}(k_1, g_1, \alpha_1, \alpha_1', x_1^-, x_1^+, x_2^-, x_2^+),$$
$$f_{1j}' = f_{1j}'(k_1^\dagger, k_1^\ddagger, g_1^\dagger, \alpha_1^\dagger, \alpha_1^\ddagger, A_1, B_1, x_1^-, x_1^+, x_2^-, x_2^+),$$
$$g_{1j}' = g_{1j}'(k_1^\dagger, k_1^\ddagger, g_1^\dagger, \alpha_1^\dagger, \alpha_1^\ddagger, A_1, B_1, x_1^-, x_1^+, x_2^-, x_2^+),$$
$$f_{2j} = f_{2j}(k_2, g_2, \alpha_2, \alpha_2', x_1^-, x_1^+, x_2^-, x_2^+),$$
$$g_{2j} = g_{2j}(k_2, g_2, \alpha_2, \alpha_2', x_1^-, x_1^+, x_2^-, x_2^+),$$
$$f_{3j} = f_{3j}(k_3, k_3', g_3, \alpha_3, \alpha_3', A_3, B_3, x_1^-, x_1^+, x_2^-, x_2^+),$$
$$g_{3j} = g_{3j}(k_3, k_3', g_3, \alpha_3, \alpha_3', A_3, B_3, x_1^-, x_1^+, x_2^-, x_2^+)$$

Since all the coefficients f_{ij} and g_{ij} of the complete elliptic integrals contain a number of terms, so that they were simply put in the compact forms. The detailed specifications are given in Choi [20].

VI. Stochastic Analysis

This section is devoted to stochastic analyses such as mean first passage time, stationary density, and stochastic bifurcation from the reduced averaged model with respect to the energy-level set of Hamiltonian H. Before such analyses, we introduce the scale and speed measure which are defined as follows:

$$S_i(H) \stackrel{\text{def}}{=} \int_{z_i}^{H} s_i(\eta)\,\mathrm{d}\eta \quad \text{and} \quad M_i(H) \stackrel{\text{def}}{=} \int_{z_i}^{H} m_i(\eta)\,\mathrm{d}\eta$$

where

$$s_i(\eta) = \exp\left\{-\int_{z_i}^{\eta} \frac{2\bar{A}_i(\xi)}{\bar{\sigma}_i^2(\xi)}\,\mathrm{d}\xi\right\}, \qquad m_i(\eta) = \frac{1}{\bar{\sigma}_i^2(\eta)s_i(\eta)}$$

and H is an interior point for each edge I_i. For $i = 3$, the lower and upper limits of integration are reversed.

In what follows, we classify the possible behavior near the boundaries b_1, b_2, b_3, and the vertex $\mathcal{O}$. According to the *Feller classification*, we find that b_1 and b_2 are classified as *entrance boundaries* whereas $b_3(H \to \infty)$ as *natural boundary*. Furthermore, we find that the vertex $\mathcal{O}$ (namely, homoclinic orbit) is accessible and the gluing condition is required to completely solve the problem. The readers are referred to Freidlin [25] and Karlin [26] for further discussion of the boundary classification.

A. Mean First Passage Time

Suppose that at time $t = 0$, the state of the system corresponds to some point defined by $H(0) = h$ within $\mathcal{D}$ which is the domain of attraction with boundary $\partial\mathcal{D}$. Let z_i be the points on the edge of the graph corresponding to the boundary $\partial\mathcal{D}$. We are interested in the time $\tau_c \stackrel{\text{def}}{=} \min\{\tau_i\}$ where $\tau_i = \inf\{t \geq 0; H(t) = z_i\}$ is the hitting time of the averaged process to the level z_i. Define the mean exit time to reach either z_1, z_2, or z_3 by the function $u(h) \stackrel{\text{def}}{=} \mathbb{E}[\tau_c : H(0) = h]$. Since the averaged process is a Markovian with the generator (44), it is calculated from the classical theory of Markov processes

$$\mathcal{L}_i^\dagger u_i(h) = \frac{1}{2}\frac{\mathrm{d}}{\mathrm{d}M_i}\left[\frac{\mathrm{d}u_i(h)}{\mathrm{d}S_i}\right] = -1, \qquad h \in \bar{\mathcal{I}}\{\mathcal{O} \qquad (54)$$

with the boundary and gluing conditions given by

$$u_i(z_i) = 0 \quad \forall\ i, \quad \text{and} \quad \sum_{i=1}^{3} (\pm)\sigma_i^2(\mathcal{O})u_i'(\mathcal{O}) = 0$$

The generator (44) is defined for continuous test functions such as $u_i(h), h \in \Gamma$. Hence, at the vertex $\mathcal{O}$ we have the continuity condition $u_1(\mathcal{O}) = u_2(\mathcal{O}) = u_3(\mathcal{O})$. The solution of Eq. (54) is given by

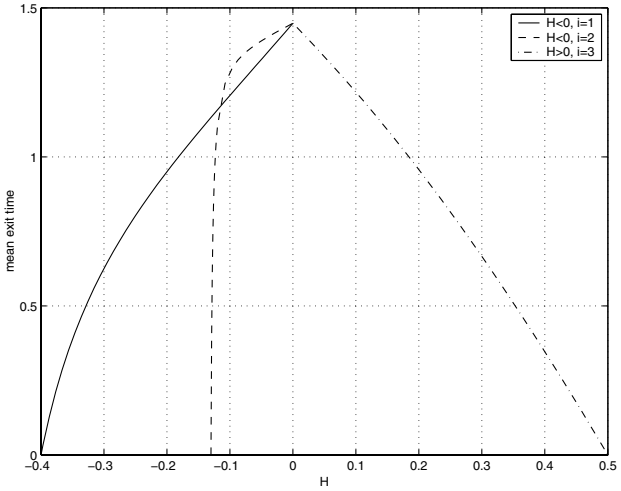

Fig. 4 Mean exit time.

$$u_i(h) = -2\int_{z_i}^{h}\left[\int_{z_i}^{\eta} m_i(\xi)\,\mathrm{d}\xi\right]s_i(\eta)\,\mathrm{d}\eta + \beta_i[S_i(h) - S_i(z_i)] + \alpha_i \qquad i = 1, 2$$
$$u_3(h) = -2\int_{h}^{z_3}\left[\int_{\eta}^{z_3} m_3(\xi)\,\mathrm{d}\xi\right]s_3(\eta)\,\mathrm{d}\eta + \beta_3[S_3(z_3) - S_3(h)] + \alpha_3 \qquad (55)$$

where h is an interior point for each edge I_i. Imposing the boundary conditions at $h = z_1, z_2$, and z_3 first yields $\alpha_i = 0$. Subsequently, the constants $\beta_i (i = 1, \ldots, 3)$ are determined from the continuity and gluing conditions at the vertex $\mathcal{O}$. The mean exit time is estimated with the set of the numerical values $\nu_1 = \nu_2 = b_0 = \mu_1 = 1$, $a_0 = -0.5$ and $\mu_2 = 0.5$ in Fig. 4. We choose the boundaries such that $z_1 = -0.4$, $z_2 = -0.13$, and $z_3 = 0.5$.

Let us conjecture the physical meanings from the numerical result. The mean first passage time can be redefined as the ensemble average of random time to exit the given boundary. As in Fig. 4 the dotted curve in leg I_2 increases very steeply and the mean exit time at the same energy level is higher than the solid curve in leg I_1. This can be interpreted by a perturbed rolling ball whose motion on the asymmetric potential curve has a more tendency toward the deeper well as the ball approaches the saddle point. Here, the position of the rolling ball would be a counterpart of the amplitude of the panel mode shapes; see Fig. 10.

B. Stationary Probability Density

It is known that if the drift and diffusion coefficients do not explicitly depend on time (time homogeneous case), then the probability distribution usually approaches a stationary distribution which is independent of the initial distribution or on time t over a long time interval. In this subsection, the stationary behavior of the reduced model is investigated through the FPE with the prescribed initial and boundary conditions. We first derive the FPE for the density with respect to energy-level set of Hamiltonian H by considering the appropriate inner product in the local coordinate H, which is defined as follows:

$$\langle f(H), g(H)\rangle_H \stackrel{\text{def}}{=} \int_H f(H)g(H)T(H)\,\mathrm{d}H \qquad (56)$$

Subsequently, we obtain the adjoint equation and boundary conditions using the fact that

$$\langle \mathcal{L}^\dagger f_i(H), g_i(H)\rangle_H = \langle f_i(H), \mathcal{L}^{\dagger *} g_i(H)\rangle_H \qquad (57)$$

Taking integration by parts gives,

$$\sum_{i=1}^{3}(\pm)\int_0^{b_i}\mathcal{L}^{\dagger}f_i(H)g_i(H)T_i(H)\,\mathrm{d}H$$
$$=\sum_{i=1}^{3}(\pm)\int_0^{b_i}\mathcal{L}^{\dagger *}g_i(H)f_i(H)T_i(H)\,\mathrm{d}H$$
$$+\sum_{i=1}^{3}(\pm)\tfrac{1}{2}\sigma_i^2(H)f_i'(H)g_i(H)\Big|_0^{b_i}+\sum_{i=1}^{3}(\pm)\{A_i(H)g_i(H)$$
$$-\tfrac{1}{2}[\sigma_i^2(H)g_i(H)]'\}f_i(H)\Big|_0^{b_i} \tag{58}$$

wherein the first term of the right hand side is defined in the form

$$(\mathcal{L}^{\dagger *}g^{\dagger})([x])\overset{\text{def}}{=}\mathcal{L}_i^{\dagger *}[g_i(H)]\overset{\text{def}}{=}-\frac{1}{T_i(H)}[A_i(H)g_i(H)]'$$
$$+\frac{1}{2}\frac{1}{T_i(H)}[\sigma_i^2(H)g_i(H)]'',\qquad [x]\in\Gamma_i \tag{59}$$

The domain of the adjoint operator is given by

$$\mathcal{D}(\mathcal{L}^{\dagger *})\overset{\text{def}}{=}\Big\{g\in C(\bar{\mathcal{I}}):\ g\in C^2(\cup_{i=1}^{3}\Gamma_i),\ \lim_{H\to H(\mathcal{O})}\mathcal{L}_i^{\dagger *}\text{exist},$$
$$\sum_{i=1}^{3}(\pm)G_i(\mathcal{O})=0,\ G_i(b_i)=0\Big\} \tag{60}$$

where $G_i(H)\overset{\text{def}}{=}A_i\ (H)g_i(H)-\frac{1}{2}[\sigma_i^2(H)g_i(H)]'$ is called probability flux or current. By introducing a probability flux $G_i(H)$, we can rewrite the FPE (59) in the simple expression,

$$\frac{\partial g_i}{\partial t}+\frac{1}{T_i(H)}(G_i)'=0 \tag{61}$$

which is called the *equation of conservation of probability*. Further, it is obvious that the stationary solutions for homogeneous FPE give rise to a constant probability flux in Eq. (61). Thus the stationary probability density is obtained by solving of the FPE

$$\mathcal{L}_i^{\dagger *}g_i=0 \tag{62}$$

subjected to the conditions that are given below.

1) The continuity of the probability density g_i:

$$g_1(\mathcal{O})=g_2(\mathcal{O})=g_2(\mathcal{O})$$

2) The probability flux at the exterior vertices is zero, which implies that the boundary conditions are reflecting, that is

$$G_i(b_i)=0,\qquad i=1,\cdots,3$$

3) The normalized probability density reads

$$\int_{b_1}^{H(\mathcal{O})}g_1(H)\,\mathrm{d}H+\int_{b_2}^{H(\mathcal{O})}g_2(H)\,\mathrm{d}H+\int_{H(\mathcal{O})}^{\infty}g_3(H)\,\mathrm{d}H=1 \tag{63}$$

The solution of Eq. (62) can be expressed in terms of the speed and scale measure as follows

$$g_i(H)=m_i(H)[C_iS_i(H)+D_i],\qquad i=1,\cdots,3 \tag{64}$$

where $m_i(H)$ and $S_i(H)$ were previously defined. The constants C_i's are determined from the given the probability flux condition, resulting in all zeros. Thus, the stationary solution becomes in the simpler forms

$$g_i(H)=\frac{D_i}{\sigma_i^2(H)}\exp\Big[2\int_{b_i}^{H}\frac{A_i(\xi)}{\sigma_i^2(\xi)}\,\mathrm{d}\xi\Big],\qquad i=1,2$$
$$g_3(H)=\frac{D_3}{\sigma_3^2(H)}\exp\Big[2\int_{H(\mathcal{O})}^{H}\frac{A_3(\xi)}{\sigma_3^2(\xi)}\,\mathrm{d}\xi\Big] \tag{65}$$

The constants D_i's are calculated through the continuity condition and the normalization condition as follows.

$$D_1=\frac{\frac{\sigma_1^2(\mathcal{O})}{\sigma_3^2(\mathcal{O})}\exp\Big[-\int_{b_1}^{0}\frac{2A_1(\xi)}{\sigma_1^2(\xi)}\mathrm{d}\xi\Big]}{D},\qquad D_2=\frac{\frac{\sigma_2^2(\mathcal{O})}{\sigma_3^2(\mathcal{O})}\exp\Big[-\int_{b_2}^{0}\frac{2A_2(\xi)}{\sigma_2^2(\xi)}\mathrm{d}\xi\Big]}{D}$$
$$D_3=\frac{1}{D} \tag{66}$$

where

$$D=\frac{\sigma_1^2(\mathcal{O})}{\sigma_3^2(\mathcal{O})}\exp\Big[-\int_{b_1}^{0}\frac{2A_1(\xi)}{\sigma_1^2(\xi)}\,\mathrm{d}\xi\Big]\int_{b_1}^{0}\frac{\exp\{\int^{H}[2A_1(\xi)/\sigma_1^2(\xi)]\mathrm{d}\xi\}}{\sigma_1^2(H)}\,\mathrm{d}H$$
$$+\frac{\sigma_2^2(\mathcal{O})}{\sigma_3^2(\mathcal{O})}\exp\Big[-\int_{b_2}^{0}\frac{2A_2(\xi)}{\sigma_2^2(\xi)}\,\mathrm{d}\xi\Big]\int_{b_2}^{0}\frac{\exp\{\int^{H}[2A_2(\xi)/\sigma_2^2(\xi)]\mathrm{d}\xi\}}{\sigma_2^2(H)}\,\mathrm{d}H$$
$$+\int_0^{\infty}\frac{\exp\{\int^{H}[2A_3(\xi)/\sigma_3^2(\xi)]\mathrm{d}\xi\}}{\sigma_3^2(H)}\,\mathrm{d}H \tag{67}$$

C. Stochastic Bifurcation

The effects of perturbation are of greatest importance near a bifurcation point in a dynamical system. In this subsection, the stochastically perturbed codimension two bifurcation associated with the double-zero eigenvalues is presented.

It is well known that stochastic bifurcation theory has two generic concepts: *Phenomenological approach* based on the Fokker–Planck equation and *dynamical approach* based on Lyapunov exponents. The former approach studies qualitative changes of probability densities p_μ which are stationary solutions of the Fokker–Planck equation. The stationary behavior of the FPE arising from a nonlinear stochastic system may, for instance, exhibit transitions from one peak to two peak or craterlike densities, which have been observed experimentally, numerically, and analytically [27–29]. The number and locations of the extrema of the stationary densities have been carefully studied. This concept can be formalized based upon the idea of Zeeman [30,31]. In brief, two probability densities p, q are equivalent ($p\sim q$) if there exist two diffeomorphisms α, β such that $p=\alpha\circ q\circ\beta$. Then the family p_μ of Fig. 5 is structurally unstable at $\mu=\mu_0$ since there exist nonequivalent densities in each neighborhood of μ_0. Accordingly, $\mu=\mu_0$ can be called a *P-bifurcation point* and such a phenomenon is called a *P bifurcation*. On the other hand, the latter approach studies bifurcations of invariant measures that are analogous to fixed points in deterministic dynamical systems. For the detailed discussion of *D bifurcation*, the readers are referred to as [32–34].

In this paper, we explore the former approach to formalize the qualitative change of the long term statistical response of the dynamical system. We examine the extrema of the stationary density (65) of the dynamical system with asymmetric bistable potential well. The solution of these extrema is found from the form

$$\frac{\mathrm{d}g_i(H)}{\mathrm{d}H}=0\Rightarrow 2A_i(H)-\frac{\mathrm{d}\sigma_i^2(H)}{\mathrm{d}H}=0,\qquad i=1,\ldots,3 \tag{68}$$

The extrema of stationary density denote, so to speak, the continuation of the deterministic constant-energy levels or limit cycles. The stability of such limit cycles is determined by the sign of $d^2g_i(H)/\mathrm{d}H^2$ at the extrema.

Numerical results of the stationary probability densities corresponding to the values of the diverse parameters μ_1, μ_2 are plotted below wherein $a_0=-1$, $b_0=\nu_1=\nu_2=1$ were adopted reasonably and the values of the exterior vertices b_1 and b_2 in Eq. (42)

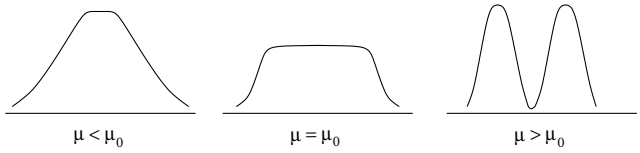

Fig. 5 Qualitative change of probability densities p_μ.

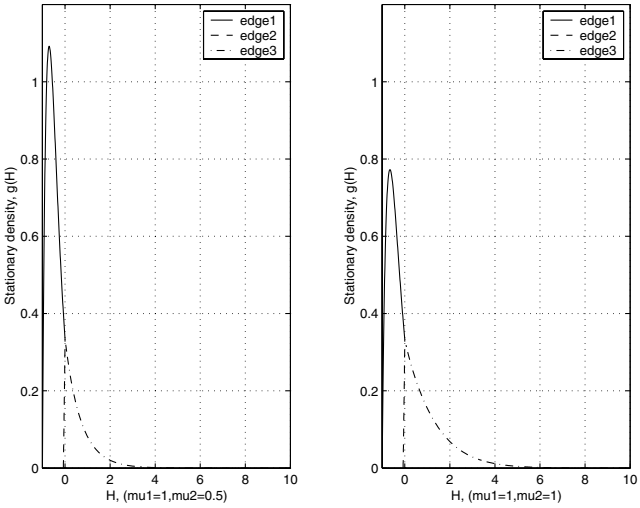

Fig. 6 Stationary probability density functions.

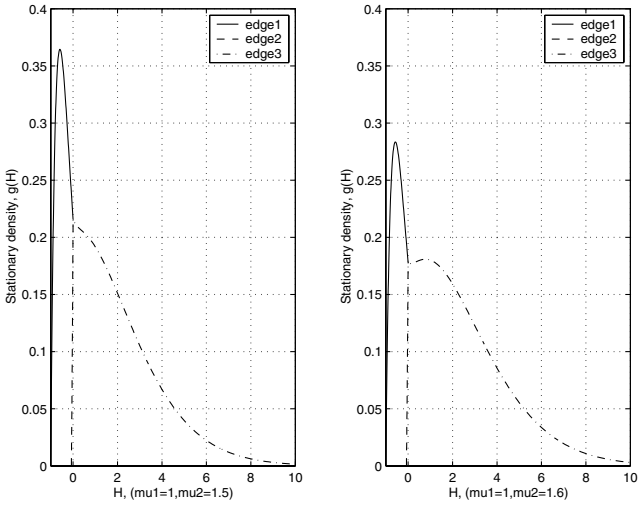

Fig. 7 Stationary probability density functions.

were determined as -1.007 and -0.08, respectively. The variation of the probability densities are given in Figs. 6–8. One of the various probability densities obtained above is sketched in three dimension for clarity in Fig. 9. It is clear that the sum of the integration with respect to the Hamiltonian for the density curve of each edge is equal to 1 as the normalization condition.

For these specific numerical values of the parameters, the P bifurcation occurs at the values of the parameters $\mu_1 = 1$ and $\mu_2 \approx 1.55$. More concretely, as the parameter μ_1 is kept constant, the densities are computed along the varying parameter μ_2, that is when $\mu_2 < 1.55$ with μ_1 being held, there exists one solution of Eq. (68) in edge I_1. On the contrary, when $\mu_2 \geq 1.55$, there exists one solution in each of edge I_1 and edge I_3. It is shown that for edge I_2 the stationary density rises up rapidly in any variation of μ_2.

According to the numerical results in Figs. 6–8, before passing a certain critical parameters' values (or the so-called stochastic P-bifurcation points), it was found that one limit cycle is formed within the reduced state space (equivalently, the set of Hamiltonians or energy levels) corresponding to the deeper well of the potential. Otherwise, two limit cycles are established within the deeper well of the potential and within the region of energy levels higher than the zero energy level corresponding to the homoclinic orbit. As mentioned earlier, the limit cycle in the sense of stochastic dynamics indicates the extremum of probability density. This means that the panel motion tends to flutter in the neighborhood of the periodic orbit which is determined by a certain energy level with the extremum of probability density curve.

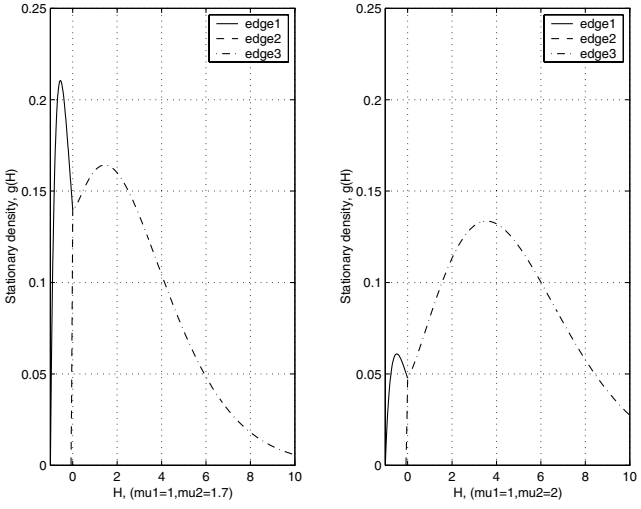

Fig. 8 Stationary probability density functions.

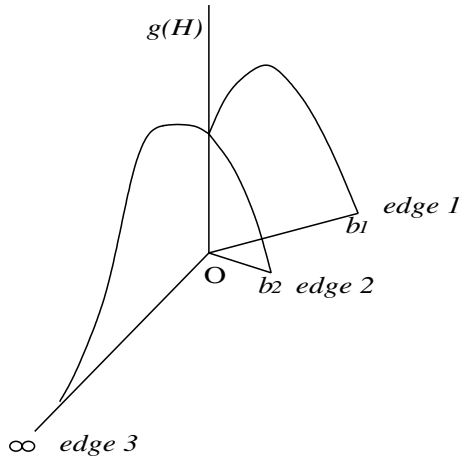

Fig. 9 Stationary probability density in three dimension ($\mu_1 = 1$, $\mu_2 = 1.7$).

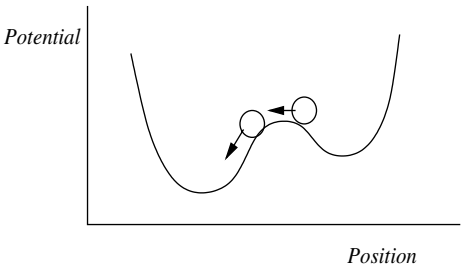

Fig. 10 The analogy of the rolling ball on the potential.

VII. Conclusions

In this paper, the effects of nonlinearities on dynamics of the flat panel in the high supersonic flow on which the TBL is imposed have been examined from the reduced-order modeling technique. Namely, in order to make the panel model analytically tractable, the following mathematical techniques were introduced. First, since it has been extremely rare to solve PDE's except for simple cases in reality, we have applied Galerkin's method with the dominant two modes to approximate the dynamical behavior of the original panel model. Second, the normal forms were fulfilled to capture the dominant nonlinearities, resulting in the simpler system along with the dimensional reduction. Finally, the nonstandard reduction through stochastic averaging was carried out so as to reduce the

randomly perturbed two-dimensional Hamiltonian system to one-dimensional limiting model. It turned out that its solution converges weakly to a Markov process on the graph with the gluing condition at vertex $\mathcal{O}$. The generator of the reduced Markov process provided probabilistic descriptions such as mean exit times and stationary probability densities. In this paper, we examined the noise-induced panel dynamics in the Phenomenological approach. In the numerical computations, it was found that P bifurcation arose at a certain critical system parameters. From the results discussed in our work, we have gained a better understanding of the mutual interaction between the nonlinearities and the turbulence in order that we might obviate the fatal consequences such as structural fatigue, fluttering, and buckling, etc. Moreover, costly aeroelastic model may be avoided by the use of the developed reduction techniques.

Acknowledgments

The authors would like to acknowledge the support of the Office of Naval Research under Grant No. N000140110647, and National Science Foundation under Grant No. CMS 00-84944.

References

[1] Dowell, E. H., "Panel Flutter: A Review of the Aeroelastic Stability of Plates and Shell," *AIAA Journal*, Vol. 8, No. 3, 1970, pp. 385–399.

[2] Dowell, E. H., and Ilgamov, M., *Studies in Nonlinear Aeroelasticity*, Springer–Verlag, New York, 1988.

[3] Dugundji, J., "Nonlinear Problems of Aeroelasticity," *Computational Nonlinear Mechanics in Aerospace Engineering*, edited by S. N. Atluri, American Institute of Aeronautics and Astronautics, New York, 1992, pp. 127–155.

[4] Namachchivaya, N. S., and Lee, A., "Dynamics of Nonlinear Aeroelastic Systems," *Journal of Aerospace Engineering*, Vol. 11, No. 2, 1998, pp. 165–174.

[5] Guckenheimer, J., and Holmes, P., *Nonlinear Oscillations, Dynamical Systems, and Bifurcations of Vector Fields*, Springer–Verlag, New York, 1983, Chap. 7.

[6] Elphick, C., Tirapegui, E., Brachet, M. E., Coullet, P., and Iooss, G., "A Simple Global Characterization for Normal Forms of Singular Vector Fields," *Physica D* Vol. 29, No. 1–2, 1987, pp. 95–127.

[7] Namachchivaya, N. S., and Sowers, R., "Stochastic Averaging of Hamitonian Systems: A Direct Martingale Proof of a Result by Khasminskii" (submitted for publication).

[8] Namachchivaya, N. S., and Sowers, R., "Stochastic Averaging of Hamiltonian Systems: A Direct Martingale Proof of a Result by Freidlin and Weber" (submitted for publication).

[9] Namachchivaya, N. S., Sowers, R. B., and Vedula, L., "Nonstandard Reduction of Noisy Duffing–van der Pol Equation," *Dynamical Systems*, Vol. 16, No. 3, 2001, pp. 223–245.

[10] Dowell, E. H., *Aeroelasticity of Plates and Shells*, Noordhoff International Publishing, Leyden, 1975, pp. 35–49.

[11] Lighthill, M. J. "Oscillating Airfoil at High Mach Number," *Journal of the Aeronautical Sciences*, Vol. 20, No. 6, 1953, pp. 402–406.

[12] Ashley, H., and Zartarian, G., "Piston Theory—A New Aerodynamic Tool for Aeroelasticians," *Journal of the Aeronautical Sciences*, Vol. 23, No. 12, 1956, pp. 1109–1118.

[13] Cunningham, H. J., "Flutter Analysis of Flat Rectangular Panels Based on Three-Dimensional Supersonic Unsteady Potential Flow," NASA R-256, Washington, DC, 1967.

[14] Bein, T., Friedmann, P., Zhong, X., and Nydick, I., "Hypersonic Flutter of a Curved Shallow Panel with Aerodynamic Heating," *AIAA/ASME/ASCE/AHS/ASC Structures, Structural Dynamics, and Materials Conference, 34th and AIAA/ASME Adaptive Structures Forum*, 1993, Technical Papers, Pts. 1–6; AIAA Paper 93-1318, 1993.

[15] Lee, A., "Nonlinear Analysis of Flat Panel Under Supersonic Flow," M.S. Thesis, University of Illinois at Urbana–Champaign, 1997.

[16] Chicone, C., *Ordinary Differential Equations with Applications*, Springer–Verlag, New York, 1999, pp. 247–274.

[17] Namachchivaya, N. S., Monica, M. M., Langford, W. F., and Evans, N. W., "Normal Form for Generalized Hopf Bifurcation with Non-Semisimple 1:1 Resonance," *Journal of Applied Mathematics and Physics (Zeitschrift fur Angewandte Mathematik und Physik)*, Vol. 45, 1994, pp. 312–335.

[18] Arnold, V. I., *Geometrical Methods of Classical Mechanics*, Springer–Verlag, New York, Heidelberg, Berlin, 1983.

[19] Wiggins, S., *Introduction to Applied Nonlinear Dynamical Systems and Chaos*, Springer–Verlag, Berlin, Heidelberg, New York, 1990, pp. 305–330.

[20] Choi, S., "Dynamics of Randomly Perturbed Nonlinear Structural and Mechanical Systems with Resonances, Ph.D. Thesis, University of Illinois at Urbana–Champaign, 2003.

[21] Karatzas, I., and Shreve, S. E., *Brownian Motion and Stochastic Calculus*, Springer–Verlag, Berlin, Heidelberg, New York, 1988, pp. 103–116.

[22] Namachchivaya, N. S., and Sowers, R., "Rigorous Stochastic Averaging at a Center with Additive Noise," *Meccanica*, Vol. 37, No. 2, 2002, pp. 85–114.

[23] Freidlin, M. I., and Wentzell, A. D., *Random Perturbations of Hamiltonian Systems*, American Mathematical Society, Providence, RI, 1994.

[24] Byrd, P. F., and Friedman, M. D., *Handbook of Elliptic Integrals For Engineers and Physicists*, Springer–Verlag, Berlin, 1954, pp. 103–134.

[25] Freidlin, M. I., and Weber, M., "Random Perturbations of Nonlinear Osillators," *The Annals of Probability*, Vol. 26, No. 3, 1998, pp. 925–967.

[26] Karlin, S., and Taylor, H. M., *A Second Course in Stochastic Processes*, Academic Press, New York, 1981, Chap. 15.

[27] Horsthemke, W., and Lefever, R., *Noise-Induced Transitions*, Springer–Verlag, Berlin/New York/Heidelberg, 1984, Chap. 7.

[28] Namachchivaya, N. S., and Leng, G., "Equivalnce of Stochastic Averaging and Stochastic Normal Forms," *Journal of Applied Mechanics*, Vol. 57, No. 4, 1990, pp. 1011–1017.

[29] Ebeling, W., Herzel, H., Richert, W., and Schimansky-Geier, L., "Influence of Noise on Duffing–Van der Pol Oscillators," *Journal of Applied Mathematics and Mechanics*, Vol. 66, No. 3, 1986, pp. 141–146.

[30] Zeeman, E., "On the Classical of Dynamical Systems," *Bulletin of the London Mathematical Society*, Vol. 20, 1988, pp. 545–557.

[31] Zeeman, E. C., "Stability of Dynamical Systems," *Nonlinearity*, Vol. 1, 1988, pp. 115–155.

[32] Arnold, L., and Boxler, P., "Stochastic Bifurcation: Instructive Examples in Dimension One," *Diffusion Precesses and Related Problems in Analysis, Vol. 2: Stochastic Flows. Progress in Probability*, edited by M. Pinsky and V. Wihstutz, Vol. 27, 1992, pp. 241–256.

[33] Xu, K., "Bifurcations of Random Differential Equations in Dimension One," *Random and Computational Dynamics*, Vol. 1, No. 3, pp. 277–305.

[34] Baxendale, P. H., *Invariant Measures for Nonlinear Stochastic Differential Equations*, Vol. 1486, Lecture Notes in Mathematics, Springer–Verlag, New York, 1990, pp. 123–140.

C. Pierre
Associate Editor